Adsorption of α-sexithiophene on Au(001): Molecule-induced partial lifting of the substrate reconstruction

Anke Höfer, Klaus Duncker, Mario Kiel, Sebastian Wedekind,* and Wolf Widdra
Institute of Physics, Martin-Luther-Universität Halle-Wittenberg, Halle, Germany
(Received 5 May 2010; revised manuscript received 21 October 2010; published 14 February 2011)

Ultrathin films of the organic molecule α-sexithiophene (6T) on Au(001) have been studied by variable-temperature scanning tunneling microscopy. Upon adsorption at room temperature, the monolayer forms two highly ordered and enantiomeric pure structures of flat-lying molecules arranged in rows. While one structural phase is related to quenching of the underlying substrate reconstruction, the quasihexagonal Au(001) reconstruction is conserved for the other one. This leads to two different substrate symmetries for the two molecular structures. Detailed analysis reveals a commensurate unit cell identical to a 6T monolayer on Ag(001) for one structure and an incommensurate 6T arrangement for the other structure strikingly similar to 6T on Au(111). *In situ* measurements at elevated temperatures show a thermally induced order-disorder transition due to molecular diffusion processes at approximately 400 K.

DOI: 10.1103/PhysRevB.83.075414 PACS number(s): 68.55.−a, 68.37.Ef, 68.43.Fg, 68.35.bd

I. INTRODUCTION

Thin films of organic molecules are used as active layers in organic electronics, for example, in organic light-emitting diodes (OLEDs) and organic field-effect transistors (OFETs). In recent years, the organic semiconducting layers in industrially crafted devices have been grown by organic vapor deposition techniques. The molecular arrangement in the organic films highly depends on the preparation conditions. As the film structure has influence on the electronic properties of the molecular layer, this also determines the device performance. Thus, the understanding and the manipulation of the molecular order are essential for optimization and reproducible production of organic devices. The organic layers are contacted by metal electrodes, where the electron-hole injection at the interface has a strong impact on device performance. Highly promising material groups with regard to their semiconducting properties are oligothiophenes and polythiophenes.[1] For systematic studies of the correlation between the structural and electronic properties, the planar, π-conjugated compounds of 4, 5, and 6 thiophene rings are especially well suited.[2–4] For characterization of the interface between the organic layer and metallic electrodes, many studies have addressed thin-film growth of 6T on metal substrates.[3,5–10] In all these studies interfacial layers with flat-lying molecules have been found. Since the first monolayer acts as a template for further growth, it might influence the order and therefore the properties of thin films. In this paper the question of how 6T adsorption influences Au(001) surface reconstruction is addressed. Although the adsorption of rigid molecules on unaltered surfaces is often observed, there are several examples in the literature that this is not stringently the case. For some studies focused on molecular adsorption on Au(111), even a lifting of the surface reconstruction is observed.[11–15] For 6T adsorption in the monolayer on Au(111), a compression but no lifting of the surface reconstruction is observed by Kiel *et al.*[9] Here we report on the details of an organic monolayer on a metallic substrate where the surface reconstruction energy is balanced by the molecule-substrate interaction. This leads to the coexistence of reconstructed and unreconstructed domains that are covered by an incommensurate and a commensurate organic monolayer, respectively. These two different molecular structures are compared with the 6T monolayer on Au(111) and Ag(001), as these two substrates are structurally very similar to the reconstructed and unreconstructed Au(001) top layer.

II. EXPERIMENTAL DETAILS

All measurements were performed under ultrahigh-vacuum conditions at a base pressure of about 10^{-10} mbar. The vacuum chamber is equipped with a homebuilt variable-temperature scanning tunneling microscope, Ar^+ ion sputtering, heating facilities, and a homebuilt Knudsen cell for 6T molecular beam deposition. The Au(001) surface was cleaned by several cycles of Ar^+ ion sputtering and subsequent annealing to 630 K for 30 min. Cleanliness and long-range order of the Au(001) surface were verified by scanning tunneling microscopy (STM). For the STM measurements electrochemically etched tungsten tips were used. The 6T molecules were evaporated onto the sample at room temperature by sublimation from a Knudsen cell at a temperature of about 500 K. A chromel-alumel thermocouple welded by a laser to the Au(001) crystal allows for accurate temperature control during STM measurements and film preparation.

III. RESULTS

Figure 1(a) shows a large-scale STM image of a one-monolayer-thick film of 6T on Au(001) recorded at an elevated surface temperature of 387 K. STM images recorded at room temperature exhibit the same structures. Figure 1(a) shows two substrate terraces with an irregularly shaped substrate step running from the lower right corner to the middle of the left side of the image. Crossing this step are two narrow but prominent areas that appear darker with respect to the color coding (gray levels). The molecules are arranged in rows, forming well-ordered domains. At first glance one can discriminate between two different structures based on the molecular row direction—one located on the main part of the terraces and the other one on the narrower prominent areas next to the step

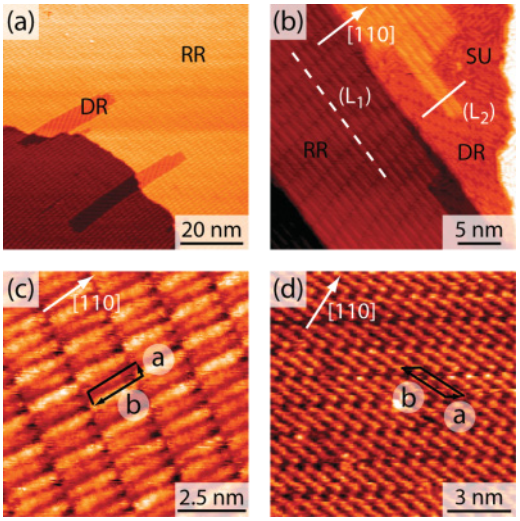

FIG. 1. (Color online) STM images of a sexithiophene monolayer on Au(001): (a) (−0.28 V, 0.9 nA, 387 K) and (b) (−0.51 V, 1.5 nA, 300 K) show two different molecular structures: rectangular row (RR) and diagonal row (DR) structure. (b) Line L_1 represents the direction of the reconstruction rows underneath RR, and L_2 runs perpendicular to the long molecular axis of RR on the upper terrace. Details of RR and DR with the corresponding unit cell are resolved in (c) (−0.36 V, 2.2 nA, 300 K) and (d) (−0.24 V, 0.7 nA, 300 K), respectively.

edge. Note the markedly long-range order of these domains, extending over several hundred square nanometers. In Fig. 1(b) an STM image at three times higher magnification is shown where the arrangement of the single rodlike molecules within the structures becomes visible. While two almost straight substrate steps run from the bottom right to the top left, another irregularly shaped one is located on the right edge of the image. The ordered 6T phase dominating on the left terrace is labeled as rectangular row structure (RR) in the following. The long axis of the 6T molecules is approximately perpendicular to the row direction in this structure. For the second structure, which is named a diagonal row structure (DR) in the following discussion, an angle of approximately 30° between the long axis of the 6T molecules and the row direction is extracted from the STM images. Details of both structures are shown in Figs. 1(c) and 1(d), respectively. In Fig. 1(b) DR is mainly observed on the right terrace. In all STM images molecules arranged in DR appear darker than molecules arranged in RR on the same terrace. Analysis of the profile along L_2 (not shown here) determines the height difference between RR and DR to (0.08 ± 0.01) nm. Following this observation we show in the subsequent discussion that the Au surface reconstruction is present below RR while it is absent underneath DR. Additionally, in Fig. 1(b) one can observe molecules (marked SU) that are not yet ordered and show statistical orientations as well as bent molecular shapes. They show the same apparent height as DR. In the high-resolution STM image of RR shown in Fig. 1(c), a fine structure of six protrusions within each molecule is visible. We explain this corrugation by the six thiophene rings within each molecule. Note that adjacent molecular rows are slightly shifted relative to each other. The rhomboidal unit cell contains one molecule and is also sketched in Fig. 1(c). Despite no intramolecular structure being visible in Fig. 1(d), the STM image clearly shows the translation along the molecular axes of adjacent molecules that leads to the observed diagonal molecular rows. The unit cell also contains only one molecule. In total we find four different molecular row directions of DR, two of them shown on the two terraces in Fig. 1(a). The molecular ordering of RR dominates, whereas DR occurs only in contact with step edges, as can be seen in Figs. 1(a) and 1(b), or next to defects of the substrate (not shown here). The boundaries between both structures on the same terrace are well defined and regularly shaped. Figure 2 displays STM images of a submonolayer 6T coverage that is prepared by annealing a 6T film with a thickness of at least one monolayer at about 410 K for several minutes. The image in Fig. 2(a) shows two different domains of DR, as well as an area displaying the rowlike reconstruction pattern of the bare Au(001) surface that coexists on the same terrace. The direction of the Au reconstruction rows deviates by about 5° from the [110] direction, as one would expect for the clean Au(001) surface as well, due to the slight rotation of the quasihexagonal top layer relative to the Au bulk.[16–20] The boundary between both DR domains, d1 and d2, runs from the substrate step in the upper-left corner to the reconstructed area almost in [100] direction. The directions of the unit-cell vectors are indicated for each domain by black solid lines, whereas the long unit-cell vector of domain d2 is perpendicular to that of domain d1. Furthermore, the long

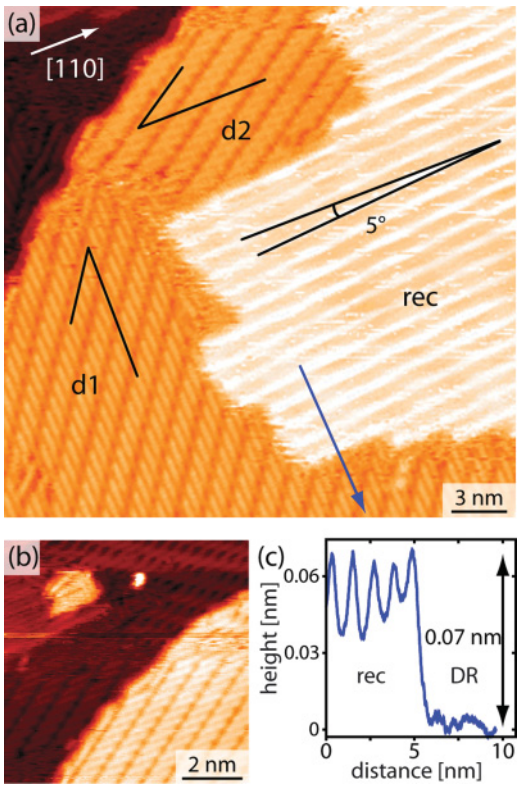

FIG. 2. (Color online) STM images upon annealing the 6T monolayer on Au(001) at 410 K. (a) The directions of the unit-cell vectors are marked by black solid lines for two mirror symmetric 6T domains, d1 and d2, of DR (−0.3 V, 1.7 nA). (b) Observation of monoatomic high Au islands upon 6T adsorption in DR (−0.3 V, 0.5 nA). (c) Line profile along the arrow indicated in (a).

unit-cell vectors and consequently, the long molecular axes are oriented in the ⟨110⟩ high-symmetry directions of the quadratic substrate. Note that both domains are mirror symmetric with respect to the [100] direction. A line profile along the blue arrow in Fig. 2(a) is shown in Fig. 2(c), where the left part corresponds to the reconstructed area and the right part to DR on the same terrace. The height difference between the maxima of the reconstruction and DR is (0.07 ± 0.01) nm, as already found in Fig. 1(b). Figure 2(b) shows an STM image of the same preparation with a substrate step running from the lower left to the upper right corner. Both terraces are covered with molecules ordered in DR. A very prominent feature of the lower terrace is the approximately 1.5-nm-wide island that is covered with unordered, rodlike 6T molecules. From line profiles the height of this island is determined to be (0.20 ± 0.01) nm, similar to a substrate step height, but only a few of these monoatomic high islands have been observed.

The unit cell of DR as determined from STM images is spanned by vectors with lengths of $a = (0.96 \pm 0.07)$ nm and $b = (2.85 \pm 0.14)$ nm with an angle of $(146.1 \pm 1.0)^\circ$ in between. The row-to-row separation of the Au(001) reconstruction rows is (1.28 ± 0.09) nm in the presence of 6T. Compared to the bare Au(001) surface reconstruction, the row-to-row separation is reduced by roughly 10%. For RR the STM images in Figs. 1(b) and 1(c) show a significant change of contrast between neighboring molecules within the same row. Along the row direction, subsequent molecules show alternating contrast with decreasing amplitude up to the point where neighboring molecules display the same color code (gray level). Beyond this point the contrast increases again. This modulation becomes even clearer in the height profile in Fig. 3, which was extracted along the molecular row direction by averaging over the width of the molecular row. Each peak in the line profile (E) corresponds to a single 6T molecule. As one would expect from the STM images, the difference between the amplitudes of adjacent peaks decreases until it is equal and then increases again. The origin of this Moiré effect

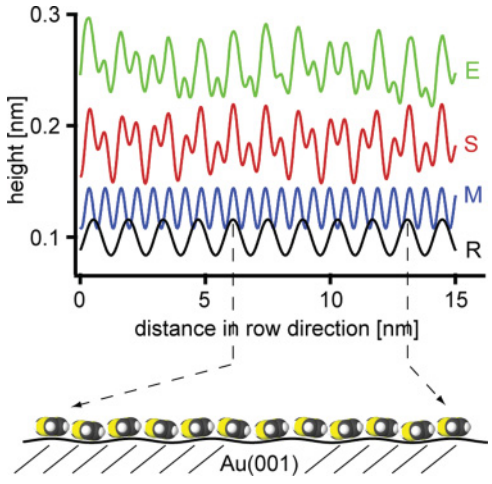

FIG. 3. (Color online) STM line profile of RR along the molecular row direction. From top to bottom: Experimentally measured profile (E), superposition (S) of the sinusoidal molecular corrugation (M), and the sinusoidal substrate corrugation (R). Lower part: Side view of a 6T molecular row on Au(001).

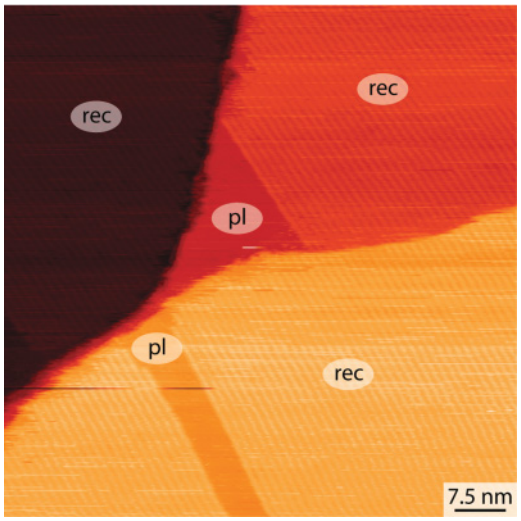

FIG. 4. (Color online) STM image of a 6T monolayer on Au(001) at an elevated surface temperature of 402 K (−0.25 V, 0.4 nA). The notations (rec) and (pl) indicate reconstructed and plain surface areas. Molecules cannot be resolved by STM due to fast molecular diffusion.

is discussed in Sec. IV. The vectors that span the unit cell of RR are determined to have lengths of $a = (0.67 \pm 0.05)$ nm and $b = (2.52 \pm 0.20)$ nm, as indicated in Fig. 1(c). Both vectors include an angle of $(98 \pm 2)^\circ$. Note that besides this specific structure, several slightly modified arrangements have been observed with small modifications in the length of the vectors and/or the included angle.

So far, the molecular structures at room temperature and at 387 K [Fig. 1(a)] have been discussed. Figure 4 shows an STM image recorded at 402 K. On the three different substrate terraces one can see large areas with the typical Au reconstruction pattern [marked (rec)] as well as plain and unstructured areas (pl) next to the step edges. In agreement with the previous considerations, the unreconstructed areas exhibit a lower apparent height than the reconstructed areas on the same terrace. Again, the boundaries between these two different surface structures are straight and oriented approximately in [−110] direction. In contrast to the STM image in Fig. 1(a) that was measured at 387 K, it is obvious that molecular structures are no longer visible by STM. From similar datasets recorded at various temperatures we derive a temperature range between 387 and 402 K in which the highly ordered 6T structures vanish. Above this transition temperature the monolayer disorders and single molecules cannot be resolved by STM due to fast diffusion.

IV. DISCUSSION

Sexithiophene adsorption on Au(001) in the monolayer regime shows two different highly ordered structures of flat-lying molecules in the all-*trans* conformation. The diagonal and the rectangular structures share a common feature in that the molecules are densely arranged in rows. If both structures are situated on the same substrate terrace, the molecules arranged in RR and those in DR show a height difference of about 0.08 nm [Fig. 1(b)], which matches the height difference between reconstructed and unreconstructed areas of the clean Au(001) surface. While for the unreconstructed

surface the Au atoms of the topmost layer are placed on hollow sites, they adopt periodically almost all positions between the hollow and on-top sites in the direction perpendicular to the reconstruction rows for the reconstructed surface. Consequently, the (20×5) reconstruction leads to a surface corrugation and an increase of the maximum surface height with respect to the unreconstructed surface of about 0.08 nm, as can be estimated from the different positions of the Au atoms perpendicular to the surface at the fourfold hollow and on-top sites. Quenching of this quasihexagonal reconstruction of the first Au layer leads to a C_{4v} symmetry of the surface layer that results in a less densely packed substrate structurally similar to Ag(001). As the packing density of the Au atoms in the quasihexagonal structure is 25% higher than for the unreconstructed surface, transport of the additional Au atoms has to occur upon quenching the Au reconstruction. The nascent excess atoms diffuse to the step edges and attach there or form Au islands on the terraces. After evaporation of 6T we indeed observe monatomic high Au islands on the surface [see Fig. 2(b)], and as compared to bare Au(001), irregularly shaped edges of the Au substrate steps [see, for example, the STM images of Figs. 1(a) and 1(b)] that stem from the addition of excess Au atoms to the formerly straight steps. From this we conclude that DR is formed concurrently with a local quenching of the substrate reconstruction, while the Au(001) reconstruction is conserved for the RR structure. This combination of RR with the corrugation of the underlying substrate reconstruction leads to the observed modulation of contrast between neighboring molecules [see Figs. 1(b) and 1(c), and profile (E) in Fig. 3]. The Fourier analysis of the line profile in Fig. 3 shows prominent peaks that correspond to the periodicity of the molecular next-neighbor distance and to the periodicity of the substrate reconstruction. Sinusoidal curves with these periodicities are depicted as the two lower solid lines (M and R, respectively) in Fig. 3. The superposition (S) of both sinusoidal curves fits well to the experimentally obtained profile (E). In conclusion, the measured molecular height modulation can be explained by the superposition of the molecular layer with an underlying substrate reconstruction such that the long molecular axis is roughly oriented along the reconstruction rows. Detailed analysis of the profile along the rows reveals that approximately 12 molecules are arranged on a distance of 5 substrate row-to-row separations as illustrated in Fig. 3(b), where the black sinusoidally shaped curve represents the surface reconstruction. In Fig. 1(b) molecules of the same height in neighboring rows are connected by the white dashed line L_1, representing the direction of the reconstruction rows underneath RR. The line coincides with the $[-110]$ direction.

The next-neighbor Au-Au distance for the unreconstructed Au(001) surface is 0.288 nm, which is almost identical to the Ag-Ag distance of the Ag(001) surface ($d_{\mathrm{NN,\,Ag(001)}} = 0.289$ nm). A commensurate unit cell for the diagonal row 6T structure described in matrix notation by

$$\begin{pmatrix} 3 & 2 \\ -10 & 0 \end{pmatrix}$$

results in unit-cell vectors of $a = 1.04$ nm and $b = 2.88$ nm, with an angle of 146.3° in between. This is in good agreement with our experimental data. There is one molecule in the unit cell that leads to a packing density of 0.60 molecules per nm^2 for DR. This structure is identical to the one found on Ag(001).[10] Following the reasoning and the experimental evidence on Ag(001), we propose a homochiral structure. Molecules of opposite chirality arrange in mirror symmetric domains. Since the substrate has fourfold symmetry, domains consisting of right- and left-handed molecules, respectively, that are rotated by 90° should exist. This consideration is verified by our experimental data.

The superstructure description for RR with respect to the quasihexagonally reconstructed Au surface layer is hindered by uncertainty about the exact structure of the Au surface layer. There are several different structural models that result in slightly different contractions of the quasihexagonal top layer in the [110] and the [-110] directions.[16,17,19,21–23] Additionally, some models propose a rotation of the top layer with respect to the bulk. Assuming a next-neighbor distance within the hexagonal top layer of $d_{\mathrm{NN}} = 0.277$ nm, which is well in the range of several structure proposals, the corresponding model of RR is depicted in Fig. 5. The molecular orientation is inclined with respect to the vector b and deviates from the high-symmetry directions. The angle between the long molecular axis and the [110] direction is estimated from the STM images to about $-(8 \pm 2)°$. One can see that molecules of adjacent rows are shifted relative to each other in such a way as to enable the ends of the molecules of one row to slide into the space between the molecules of the adjacent row. The molecule-substrate interaction seems to be only weakly site specific, which points to an incommensurate nature of RR. So, from an energy-related point of view, a maximization of the molecule packing density balanced by the intermolecular forces is favorable. A more detailed knowledge of the hexagonal top layer of the bare Au(001) surface is not necessary for an improved description of the molecular superstructure, because the formation of RR influences the Au top layer underneath. As shown by line L_1 in Fig. 1(b), the reconstruction rows are oriented in the ⟨110⟩ directions, in contrast to a reconstructed Au surface without molecular structures (see Fig. 2). From this we conclude that the rotation of the hexagonal Au top layer is lifted. Additionally, the formation of RR might also change the interatomic distances. For monolayer adsorption of 6T/Au(111), Kiel *et al.* found a slightly enlarged periodicity of the herringbone reconstruction with respect to the bare surface.[9] The assumption of somewhat different modifications of the hexagonal top layer for different substrate areas can

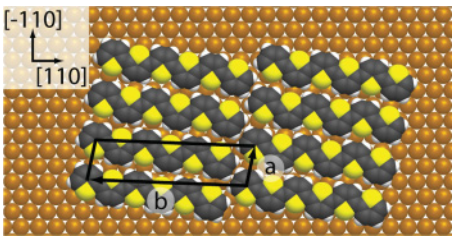

FIG. 5. (Color online) Calotte model for the incommensurate RR of 6T on the quasihexagonally reconstructed Au(001) surface. The observed superstructure is similar to that found for 6T on Au(111).[9] Note that the illustrated domain consists of right-handed 6T molecules.

explain the observation of several slightly different coexisting rectangular row structures on Au(001). Apart from that, it is apparent that RR observed on Au(001) has a striking similarity to the dominating molecular 6T structure found on Au(111). Kiel *et al.* report a monolayer unit cell with the dimensions $a = (0.61 \pm 0.06)$ nm, $b = (2.4 \pm 0.2)$ nm, and an angle of $(95 \pm 1)^\circ$ in between.[9] On Au(111) this structure has been identified as point-on-line induced, which also seems to be the driving force for Au(001). The bare Au(111) surface has a next-neighbor distance of about 0.275 nm that deviates by not more than 1% from the next-neighbor distance of the hexagonally reconstructed Au(001) surface discussed here. Due to the small unit cell and following the argumentation for Au(111), we assume homochiral domains as well for 6T RR on Au(001). For the same reasons as discussed in detail by Kiel *et al.*, only a homochiral packing of the molecules allows for the observed optimized two-dimensional packing based on the superstructure analysis.[9] This maximization of the packing density seems to be the driving force for the final monolayer structure. In contrast to Au(111), the bulk underneath the hexagonal top layer of Au(001) has a square symmetry that results in two reconstruction domains. Since for Au(001) the rotation of the hexagonal top layer is lifted underneath RR, the fourfold bulk structure results in only two different domains of a certain handedness rotated by 90° relative to each other. The domains of opposite handedness are obtained by reflection at the mirror plane, which includes the surface normal and either the [110] or the [−110] direction.

The observed commensurability of DR is the result of the preponderance of the molecule-substrate interaction relative to the intermolecular interaction. In contrast, the incommensurability of RR suggests an only weakly site-specific arrangement of the molecules. This indicates that molecules in DR are bound more tightly to the surface. The binding energy for molecules in DR is larger than for molecules in RR: $E_{DR} > E_{RR}$. In agreement with the observations for several other adsorbate-covered surfaces, the adsorption on a structurally more open surface is typically stronger.[24–26] This observation seems to contradict the second observation that the RR structure is the favored one and that DR is only present at steps or defects [Figs. 1(a) and 1(b)]. We rationalize both findings in the qualitative energy diagram shown in Fig. 6. The three energy levels in the upper part illustrate the relative energies of the bare Au(001) surface for the case of an unreconstructed (1 × 1) top layer, for the reconstructed quasihexagonal (20 × 5) structure, and for the reconstructed (20 × 5) structure in the presence of defects. Starting from the (1 × 1) surface, the surface free energy is lowered by ΔE_{rec} upon (20 × 5) reconstruction. This is in line with the observation that the clean unreconstructed (1 × 1) surface is only metastable and the quasihexagonal reconstruction is thermodynamically preferred. In the presence of defects the free energy is higher by the sum of the defect creation energies. On these three surfaces the 6T monolayer adsorbs either in DR or RR with binding energies of E_{DR} and E_{RR}, respectively. The total surface free energy upon 6T monolayer adsorption for the different structures is sketched in the lower part of Fig. 6. In the following we assume that near defects or near step edges the surface reconstruction is slightly less favored as compared to that on large, ideal terraces, as illustrated on the right side of Fig. 6. From the dominant formation of RR we conclude that as indicated in Fig. 6, the difference between the adsorption energies per area for molecules in the DR and the RR structure is smaller than the free energy difference of the unreconstructed and the quasihexagonal reconstructed Au(001) surface. In contrast, next to defects because of the lowered (slightly unfavored) reconstruction energy, the total energy is less favored as compared to an reconstructed Au top layer covered by a DR monolayer, as shown on the right side of Fig. 6. The evolving (1 × 1) Au surface structure is stabilized by the difference in the 6T binding energies on unreconstructed and reconstructed parts of the surface, E_{DR} and E_{RR}, respectively.

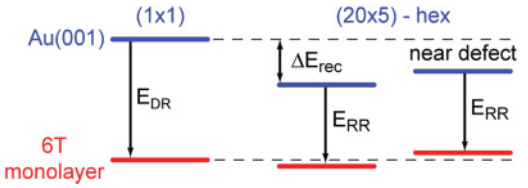

FIG. 6. (Color online) Relative energies of the bare and 6T covered Au(001) for an unreconstructed (1 × 1) surface (left) and a quasihexagonally reconstructed surface (middle and right). Note the different reconstruction energies for reconstruction on large defect-free terraces (middle) and next to defects (right).

Our findings of slightly different reconstruction energies at different parts of the terraces are confirmed by *in situ* STM measurements at the Au(001) electrolyte interface. Kolb *et al.* show that the lifting of the surface reconstruction exclusively starts at defects of the surface.[25] For defect-free terraces the step edges serve as starting points. Consequently, there is a strong influence of the step distribution on the transition kinetics. The transformation from the quasihexagonal to a quadratic top layer proceeds rather anisotropically.[25] Although the kinetics of the (hex) → (1 × 1) transition were observed in an electrolytic environment, we expect similar processes and kinetics here. The experimental observation that after annealing the monolayer up to (395 ± 8) K the RR structure, in contrast to DR, is not restored after cooling to room temperature is discussed in the following section. Based on the line profile presented in Fig. 2(c), we show that both the reconstructed as well as the unreconstructed part of the surface are covered with 6T molecules. Kilian *et al.* determined the average vertical bonding distance of flat-lying end-capped α-quarterthiophene from an Ag(111) surface to about (0.315 ± 0.005) nm.[27] Based on the similarity of both systems, we expect a similar vertical bonding distance for 6T on Au(001). Ignoring additional electronic effects, one would expect apparent step heights of approximately 0.3 and 0.2 nm for one organic layer or one additional Au layer, respectively. The line profile in Fig. 2(c) displays a height difference of only 0.07 nm between the reconstructed surface areas and DR, which rules out the absence of the organic layer. In fact, the height difference is similar to the value observed in Fig. 1(b) for 6T monolayers on reconstructed and unreconstructed Au(001). These observations can only be explained by the presence of a 6T layer on the reconstructed areas. There the molecules diffuse too fast to be imaged by STM at room temperature. Following the schematics of Fig. 6, the weaker

TABLE I. Comparison of the two different 6T structures on Au(001): the diagonal and the rectangular row structure.

	Diagonal row structure	Rectangular row structure
Au(001) top layer	Unreconstructed (1 × 1)	Quasi-hexagonal
6T structure	Commensurate, homochiral	Incommensurate, homochiral
Long molecular axis	Parallel to ⟨110⟩	Deviates from ⟨110⟩
Unit cell; molecular density	Well defined; 0.60 nm^{-2}	Small structural variations result in (0.63 ± 0.06) nm^{-2}
Diffusion onset	(395 ± 8) K	(395 ± 8) K

adsorbate-substrate interaction E_{RR} on the reconstructed Au(001) surface also suggests a lower diffusion barrier there. Additionally, for coverage below a fully saturated monolayer one expects preferred saturation on unreconstructed areas of the Au(001) surface, since the molecules there experience larger binding energy. Upon annealing to 395 K, thermal desorption and/or dewetting processes occur. This reduces the local coverage on the reconstructed areas and enables fast diffusion of the molecules there. This observation emphasizes the expected weaker bonding of 6T on the reconstructed substrate compared to the stronger bonding of DR on the unreconstructed Au(001)-(1 × 1). The different properties of the two 6T structures on Au(001) are summarized in Table I.

V. CONCLUSION

Upon adsorption of α-sexithiophene on Au(001), the quasihexagonal surface reconstruction of Au(001) is partly quenched. On the unreconstructed areas, which reveal a (1 × 1) substrate structure, the 6T monolayer forms a commensurate diagonal row structure. Its unit cell can be described in matrix notation by

$$\begin{pmatrix} 3 & 2 \\ -10 & 0 \end{pmatrix}.$$

At submonolayer 6T coverages, in addition to the diagonal row structure, reconstructed areas with fast-diffusing molecules also exist. The increase of the coverage of up to one monolayer leads to the formation of densely packed molecular rows conserving the underlying substrate reconstruction. This molecular arrangement is incommensurate with respect to the substrate and has a striking similarity to the molecular structure of 6T on Au(111). There, a point-on-line stabilization of the incommensurate layer is found, which we expect to be relevant here as well.[9] STM measurements at elevated temperatures show that the coexistence of reconstructed and unreconstructed areas is conserved, whereas well-ordered molecular structures cannot be imaged due to fast molecular diffusion. A sharp transition temperature for the onset of this diffusion can be observed at (395 ± 8) K. Upon annealing above this transition temperature the rectangular row structure disappears on the reconstructed Au(001), whereas the diagonal row structure is restored on the unreconstructed Au(001). The absence of visible molecular structures on the reconstruction is explained by diffusion due to a reduced local coverage there, caused by desorption or dewetting, for example.

ACKNOWLEDGMENTS

This work was supported by the Deutsche Forschungsgemeinschaft through SFB 418. Furthermore, we gratefully acknowledge Ralf Kulla for technical support.

*Present address: Max-Planck-Institut für Mikrostrukturphysik, Halle, Germany

[1] G. Witte and C. Wöll, J. Mater. Res. **19**, 1889 (2004).
[2] C. Ziegler and D. Fichou, *Handbook of Oligo- and Polythiophenes* (Wiley-VCH, NewYork, 1999).
[3] A. Soukopp, K. Glöckler, P. Kraft, S. Schmitt, M. Sokolowski , E. Umbach, E. Mena-Osteritz, P. Bäuerle, and E. Hädicke, Phys. Rev. B **58**, 13882 (1998).
[4] P. Bäuerle, Adv. Mater. **4**, 102 (1992).
[5] S. Prato, L. Floreano, D. Cvetko, V. De Renzi, A. Morgante , S. Modesti, F. Biscarini, R. Zamboni, and C. Taliani, J. Phys. Chem. B **103**, 7788 (1999).
[6] M. Kiguchi, G. Yoshikawa, and K. Saiki, J. Appl. Phys. **94**, 4866 (2003).
[7] A. Mäkinen, J. Long, N. Watkins, and Z. Kafafi, J. Phys. Chem. B **109**, 5790 (2005).
[8] H. Inoue, G. Yoshikawa, and K. Saiki, Jpn. J. Appl. Phys., Part 1 , **45**, 1794 (2006).
[9] M. Kiel, K. Duncker, C. Hagendorf, and W. Widdra, Phys. Rev. B **75**, 195439 (2007).
[10] K. Duncker, M. Kiel, A. Hoefer, and W. Widdra, Phys. Rev. B **77**, 155423 (2008).
[11] E. I. Altman, and R. J. Colton, Surf. Sci. **279**, 49 (1992).
[12] W. P. Fitts, J. M. White, and G. E. Poirier, Langmuir **18**, 1561 (2002).
[13] J. K. Gimzewski, S. Modesti, T. David, and R. R. Schlittler, J. Vac. Sci. Technol. B **12**, 1942 (1994).
[14] P. Maksymovych, D. C. Sorescu, and J. T. Yates, Phys. Rev. Lett. **97**, 146103 (2006).
[15] G. E. Poirier and E. D. Pylant, Science **272**, 1145 (1996).
[16] G. K. Binnig, H. Rohrer, C. Gerber, and E. Stoll, Surf. Sci. **144**, 321 (1984).
[17] K. Yamazaki, K. Takayanagi, Y. Tanishiro, and K. Yagi, Surf. Sci. **199**, 595 (1988).
[18] D. L. Abernathy, S. G. J. Mochrie, D. M. Zehner, G. Grübel, and D. Gibbs, Phys. Rev. B **45**, 9272 (1992).
[19] S. G. J. Mochrie, D. M. Zehner, B. M. Ocko, and D. Gibbs, Phys. Rev. Lett. **64**, 2925 (1990).
[20] Y. Samson, S. Rousset, S. Gauthier, J. C. Girard, and J. Klein, Surf. Sci. **315**, L969 (1994).

[21]D. G. Fedak and N. A. Gjostein, Surf. Sci. **8**, 77 (1967).
[22]K. H. Rieder, T. Engel, R. H. Swendsen, and M. Manninen, Surf. Sci. **127**, 223 (1983).
[23]F. Ercolessi, E. Tosatti, and M. Parrinello, Phys. Rev. Lett. **57**, 719 (1986).
[24]G. A. Somorjai and M. A. Van Hove, Prog. Surf. Sci. **30**, 201 (1989).
[25]D. M. Kolb, Prog. Surf. Sci. **51**, 109 (1996).
[26]D. M. Kolb, Surf. Sci. **500**, 722 (2002).
[27]L. Kilian, W. Weigand, E. Umbach, A. Langner, M. Sokolowski, H. L. Meyerheim, H. Maltor, B. C. C. Cowie, T. Lee, and P. Bäuerle, Phys. Rev. B **66**, 075412 (2002).